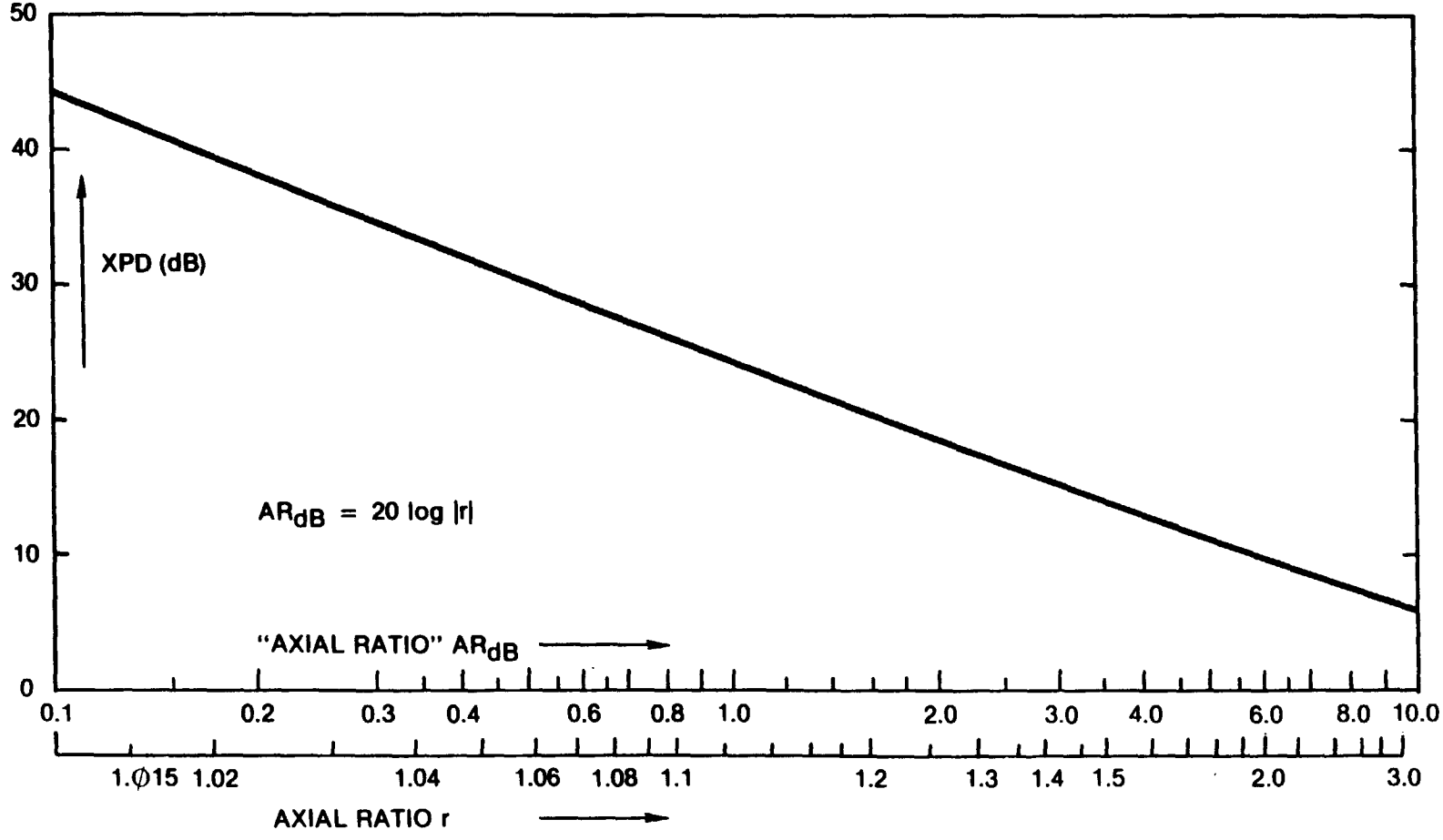


Figure 4.2-4. XPD vs. Axial Ratio of Elliptically Polarized Wave (LHCP is Copolarized)

Isolation, I, is defined as the ratio of the output power available at the antenna's "copolarized" port ($P_c$) to the output power at the "crosspolarized" port ($P_x$). The polarization states coupled to the "copolarized" and "crosspolarized" ports are $a_c$ and $a_x$, respectively. Since the antenna is non-ideal, $a_c$ and $a_x$ are not necessarily orthogonal, and $a_c$ does not necessarily correspond to the pure copolarized state. Denoting the state of the received wave as w' and the wave's power flux density as $S_w'$, we have from (4.2-11):

$$I = 10 \log \frac{P_c}{P_x} = 10 \log \frac{S_{w'} A_e m_p(w',a_c)}{S_{w'} A_e m_p(w',a_x)}$$

$$= 10 \log \frac{m_p(w',a_c)}{m_p(w',a_x)} \qquad (4.2\text{-}23)$$

It is useful to be capable of finding XPD in terms of I, which is measurable. The power available at the "copolarized" antenna port can be written in terms of the true copolarized and crosspolarized wave components, w and $w_o$.

$$P_c = A_e \left[ S_w m_p(w,a_c) + S_{w_o} m_p(w_o,a_c) \right] \qquad (4.2\text{-}24)$$

Likewise for the "crosspolarized" power

$$P_x = A_e \left[ S_w m_p(w,a_x) + S_{w_o} m_p(w_o,a_x) \right] \qquad (4.2\text{-}25)$$

$S_w$ and $S_{w_o}$ are the power flux density in the true copolarized and crosspolarized states, respectively. Now we have

$$I = 10 \log \frac{S_w m_p(w,a_c) + S_{w_o} m_p(w_o,a_c)}{S_w m_p(w,a_x) + S_{w_o} m_p(w_o,a_x)}$$

$$= 10 \log \frac{(xpd)m_p(w,a_c) + m_p(w_o,a_c)}{(xpd)m_p(w,a_x) + m_p(w_o,a_x)} \qquad (4.2\text{-}26)$$

where $xpd = S_w/S_{w_o} = \log^{-1}(XPD/10)$

Since the "copolarized" state of the antenna is assumed to be well-matched to the true copolarized wave component,

$$m_p(w_o,a_c) << m_p(w,a_c)$$

So this term is negligible and

$$I = 10 \log \frac{m_p(w,a_c)}{m_p(w,a_x) + m_p(w_o,a_x)/(xpd)} \qquad (4.2\text{-}27)$$

Note that when the antenna is nearly ideal,

$$m_p(w,a_c) = 1,\ m_p(w_o,a_x) = 1,\ m_p(w,a_x) = 0$$

and so I = XPD. On the other hand, when the XPD is very high,

$$I = 10 \log [m_p(w,a_c)/m_p(w,a_x)]$$

which is a function of the antenna only. This implies that a given antenna can be used to measure XPD to a given accuracy up to a certain maximum XPD value which is determined by the antenna performance parameters.

For the CP case, the equation for I becomes

$$I = 10 \log \frac{\frac{1}{2} + \frac{r_c}{r_c^2 + 1}}{\frac{1}{2}(xpd^{-1}+1) + \frac{r_x}{r_x^2 + 1}(xpd^{-1}-1)} \qquad (4.2\text{-}29)$$

where $r_c$ and $r_x$ are the axial ratios of the antenna's "copolarized" and "crosspolarized" states, respectively. Figure 4.2-5 shows I versus XPD for various values of axial ratio $AR_{dB}$. The "copolarized" and "crosspolarized" axial ratios are made equal in the figures, but I is actually nearly independent of $r_x$. The figure gives the amount of error to be expected when measuring XPD.

For the LP case, we obtain

$$I = 10 \log \frac{1 + Q_c \cos 2\tau_c}{(1 + xpd^{-1}) - (1-xpd^{-1}) Q_x \cos 2(\tau_x - 90°)} \qquad (4.2\text{-}30)$$

where $Q_{c,x} = (r_{c,x}^2 - 1)/(r_{c,x}^2 + 1)$

$\tau_{c,x}$ = antenna "copolarized", "crosspolarized" axis orientation angle

$r_{c,x}$ = antenna "copolarized", "crosspolarized" axial ratio

The copolarized wave axis is taken as the reference for the antenna axis orientation angles. Figures 4.2-6 and 4.2-7 show I versus XPD for various antenna axial ratios and axis misalignment angles. The first figure is for perfect axis alignment and varying axial ratio. As with the CP case, equal axial ratios for the "copolarized" and "crosspolarized" states were assumed, but isolation is practically independent of the "copolarized" axial ratio, $r_c$, when it is large (>20dB). Figure 4.2-7 shows the effect of axis misalignment for the $AR_{dB}$=30dB case. The antenna axes are assumed orthogonal, with $\tau_x = \tau_c - 90°$, but the isolation is not strongly dependent on $\tau_c$ for $\tau_c < 10°$.

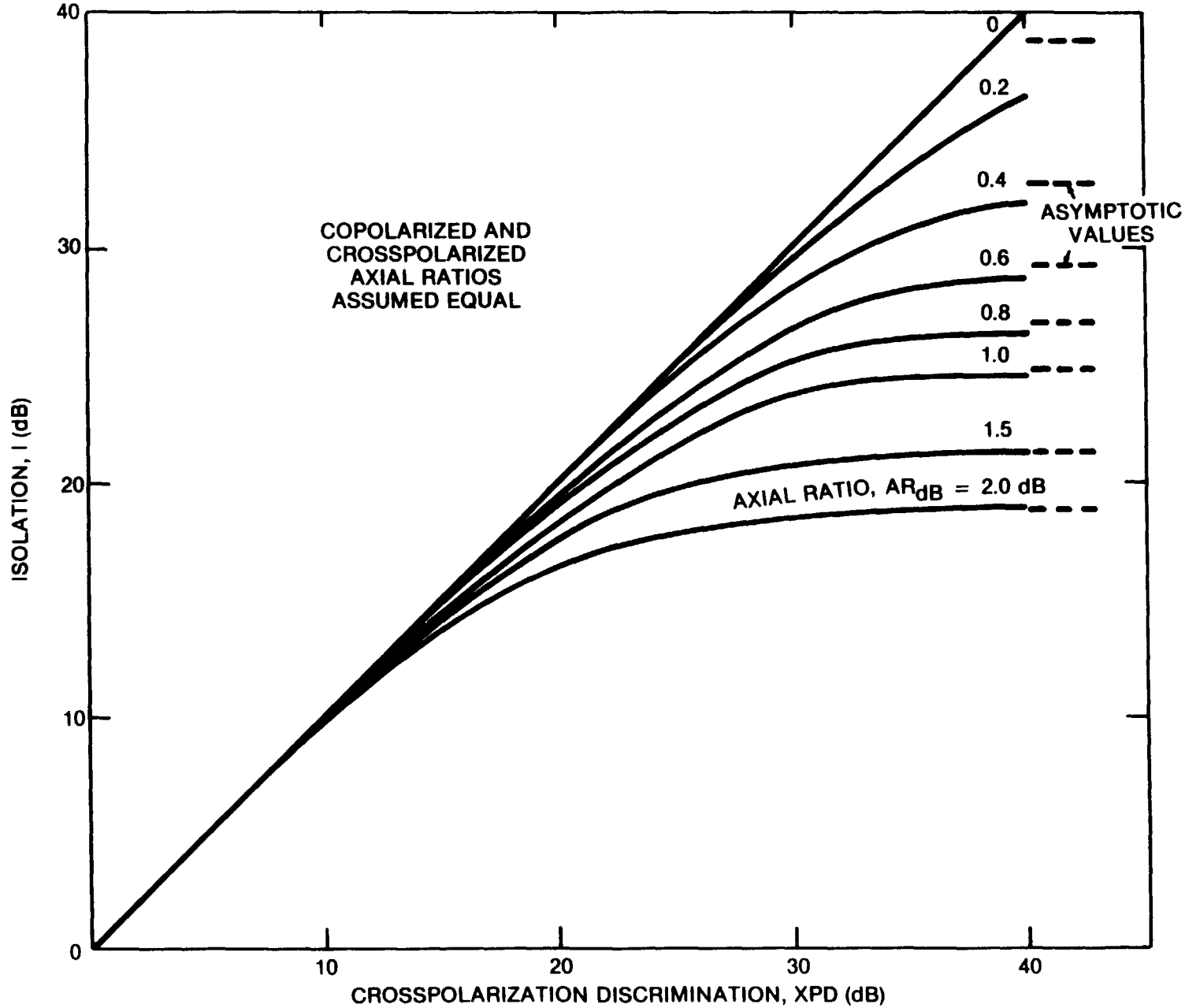


Figure 4.2-5. XPD and Antenna Axial Ratio - Circular Polarized Case

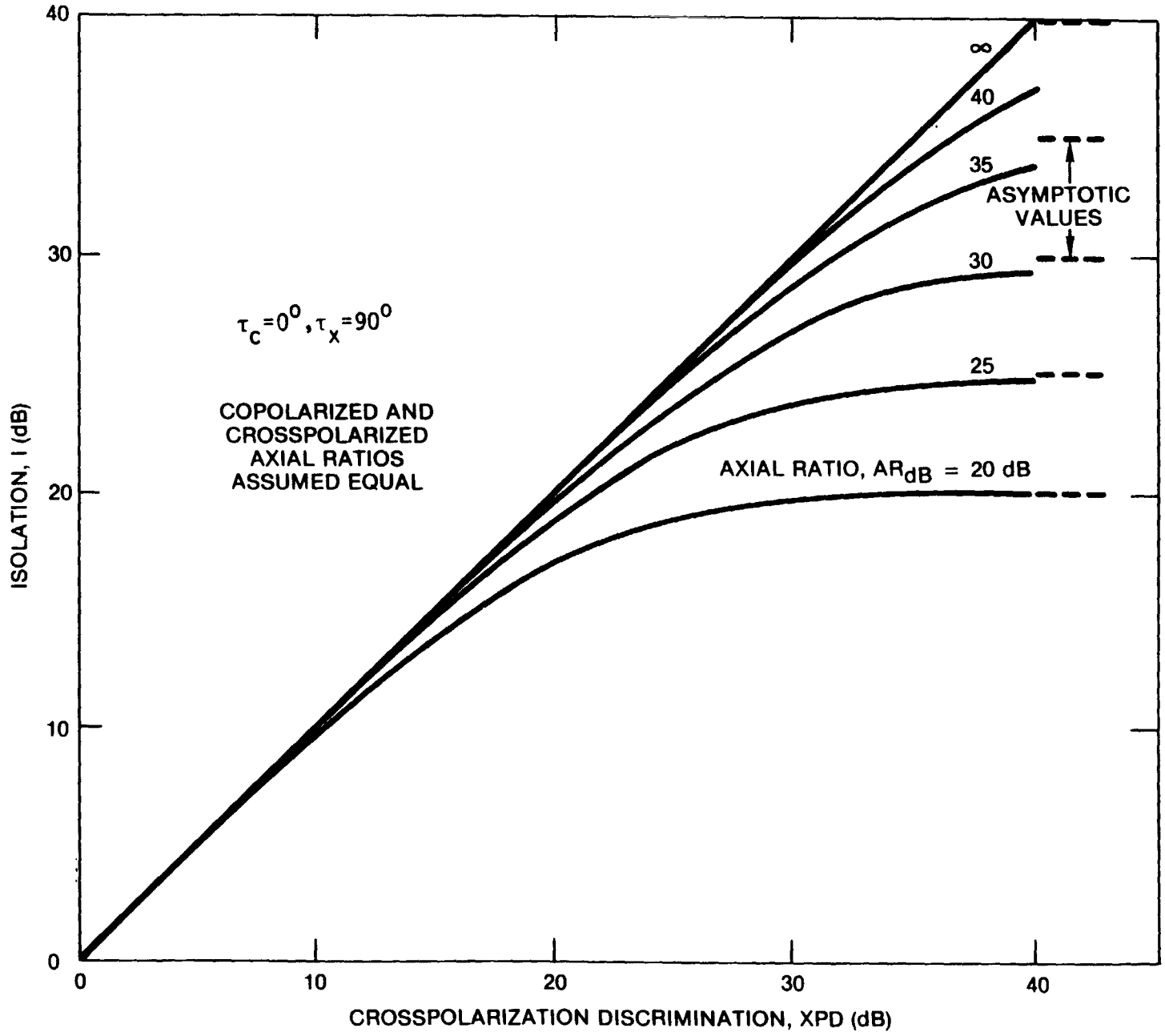


Figure 4.2-6. Isolation vs. XPD and Antenna Axial Ratio - Linear Polarized Case, No Angle Misalignment

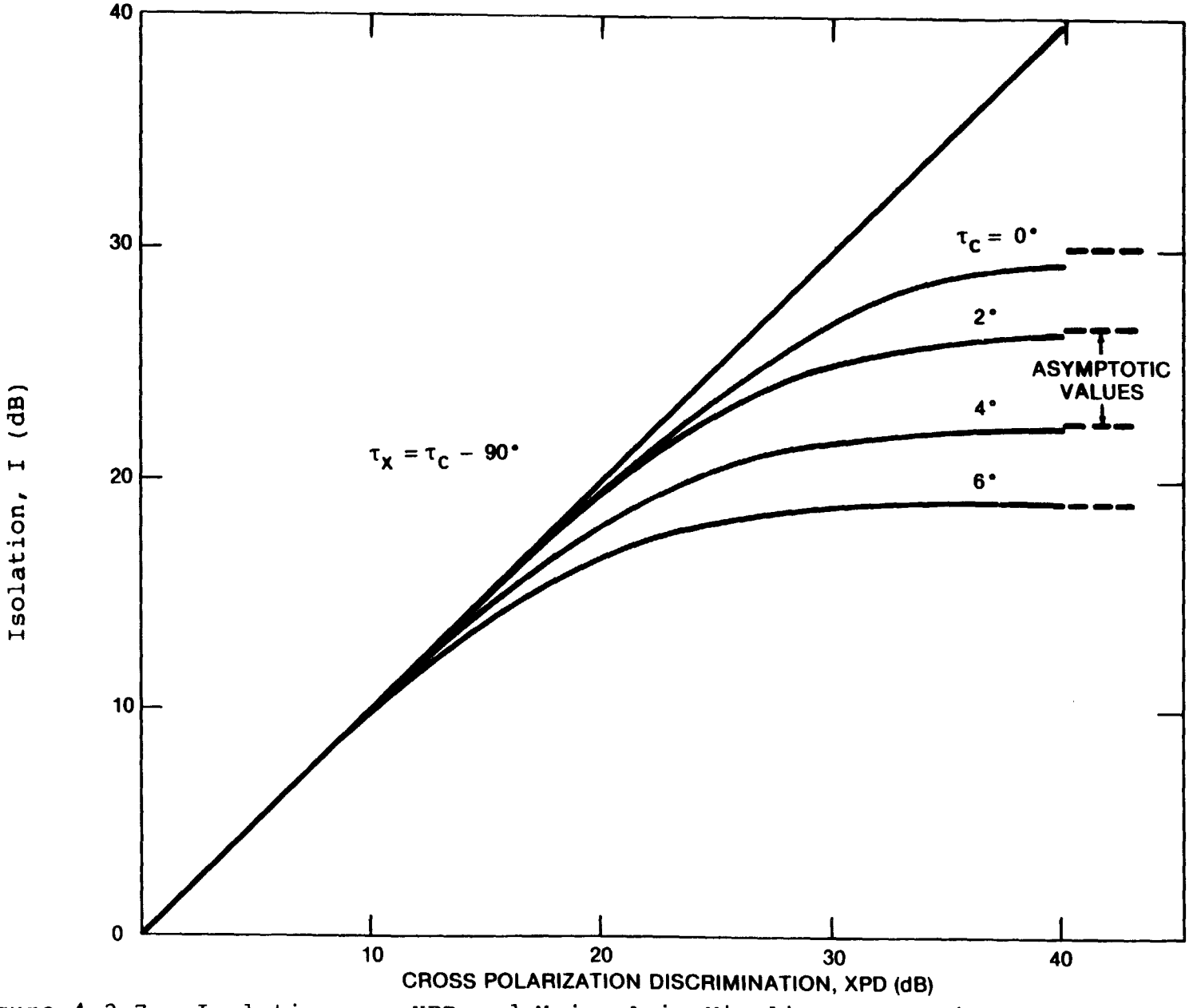


Figure 4.2-7. Isolation vs. XPD and Major Axis Misalignment - Linear Polarized Case, Axial Ratio, $AR_{dB}$=30dB

## 4.3 RAIN DEPOLARIZATION

### 4.3.1 Theory of Rain Depolarization

Rain depolarization can be modelled using the same techniques applied to rain attenuation. The essential difference is that in examining depolarization, the raindrops are assumed to be oblate spheroids. The attenuation analysis assumed that the raindrops were spherical. Figure 4.3-1 shows the geometry for a dual LP wave incident on an oblate spheroidal raindrop. The raindrop is at an arbitrary orientation with respect to the direction of propagation of the wave. The orientation is specified by the angle q, between the propagation vector and the raindrop's symmetry axis. The plane containing α will be referred to as the plane of incidence.

$E_x$ and $E_y$ are electric field vectors of two orthogonal LP waves. They are in a plane normal to the propagation vector, and each one can be resolved into two components: a component in the plane of incidence, and a component normal to it. Parallel to these components, we define two symmetry axes, labeled I and II in the figure. The projection of the raindrop into the plane containing the electric field vectors is an ellipse, and axes I and II are its minor and major axes, respectively. Figure 4.3-2 shows this ellipse and how the electric fields are resolved into their "I" and "II" components.

The total electric field magnitudes in the I and II directions ($E_I$ and $E_{II}$) are given by

$$\begin{bmatrix} E_I \\ E_{II} \end{bmatrix} = \begin{bmatrix} \cos\theta & -\sin\theta \\ \sin\theta & \cos\theta \end{bmatrix} \begin{bmatrix} E_x \\ E_y \end{bmatrix} = R \begin{bmatrix} E_x \\ E_y \end{bmatrix} \qquad (4.3\text{-}1)$$

where θ, the canting angle, is the angle between the x and I axes.

Now consider a region of space containing many identical raindrops with the same orientation distributed throughout it. According to scattering theory, the effect of many scatterers along

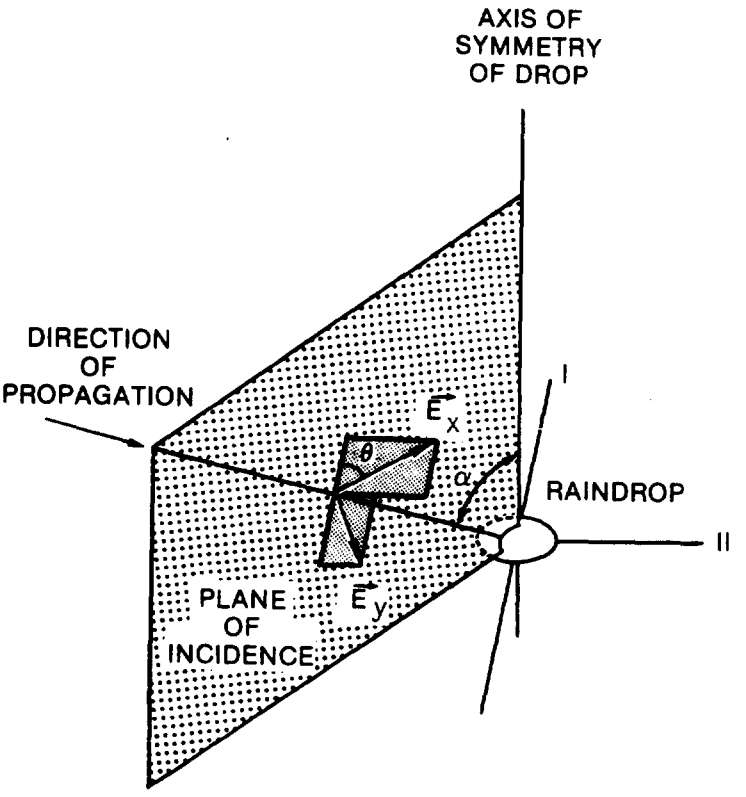


Figure 4.3-1. Geometry for Rain Depolarization Analysis

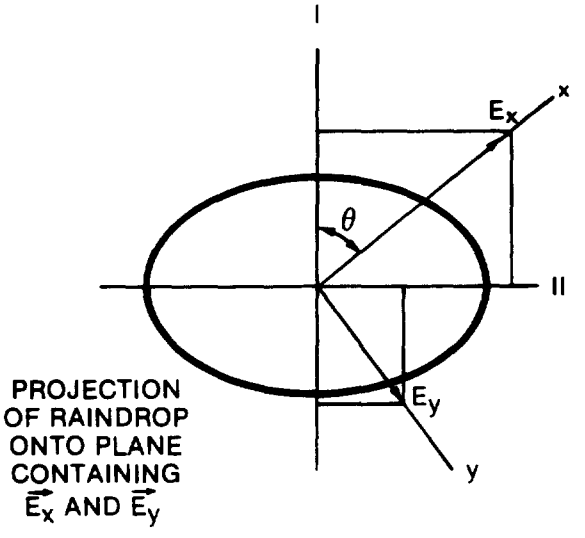


Figure 4.3-2. Resolution of Electric Fields into I and II Components

the propagation path of a wave is to multiply the electric field vector by a transmission coefficient of the form

$$T = \exp[-(a-j\Phi)L] \qquad (4.3\text{-}2)$$

where L is the path length through the scattering region. The a term of the exponent produces attenuation of the wave, and $\Phi$ produces a phase lag. This phase lag is in addition to the normal free-space phase retardation of the fields. Instead of a and $\Phi$, which have units of nepers per unit length and radians per unit length, respectively, the more useful parameters, A and $\underline{\Phi}$, are normally used:

A = specific attenuation of power flux density of wave, in dB/km.

$$= 20(\log_{10}e)a = 8.686\ a$$

$\underline{\Phi}$ = specific phase lag of wave, in degrees/km.

$$= (180/\pi)\ \Phi$$

A region filled with oblate spheriodal raindrops must be characterized by two transmission coefficients: $T_I$, applied to the "I" component of the electric field, and $T_{II}$, applied to the "II" component. Denoting the fields of the wave incident on the scattering region by a subscript i, and the fields of the wave exiting the region by s (for scattered), we can write

$$\begin{bmatrix} E_{Is} \\ E_{IIs} \end{bmatrix} = \begin{bmatrix} T_I & 0 \\ 0 & T_{II} \end{bmatrix} \begin{bmatrix} E_{Ii} \\ E_{IIi} \end{bmatrix} = T \begin{bmatrix} E_{Ii} \\ E_{IIi} \end{bmatrix} \qquad (4.3\text{-}3)$$

Now the coordinate rotation R, defined above, can be applied to get an equation for the effect of the scattering region on the field vectors in the x and y directions.

$$\begin{bmatrix} E_{xs} \\ E_{ys} \end{bmatrix} = R^{-1} T R \begin{bmatrix} E_{xi} \\ E_{yi} \end{bmatrix} = T' \begin{bmatrix} E_{xi} \\ E_{yi} \end{bmatrix} \qquad (4.3\text{-}4)$$

Figure 4.3-3 shows how the three component transformations are successively applied to produce T'. The overall transformation matrix T' can be evaluated to yield

$$T' = \begin{bmatrix} t_{xx} & t_{xy} \\ t_{yx} & t_{yy} \end{bmatrix}$$

$$\begin{aligned} t_{xx} &= T_{\parallel} \cos^2\theta + T_{\perp} \sin^2\theta \\ t_{yy} &= T_{\parallel} \sin^2\theta + T_{\perp} \cos^2\theta \\ t_{xy} &= t_{yx} = \frac{1}{2}(T_{\parallel} - T_{\perp}) \sin^2\theta \end{aligned} \qquad (4.3\text{-}5)$$

Chu (1974) gives expressions for these parameters in terms of the As and $\Phi$s.

Calling the LP wave polarized in the x direction the copolarized wave, we can now obtain expressions for the XPD:

$$\begin{aligned} XPD_x &= 10 \log \frac{|E_{xs}|^2}{|E_{ys}|^2} \quad \text{with } E_{yi} = 0 \\ &= 10 \log \frac{|t_{xx}|^2}{|t_{yx}|^2} \\ &= 20 \log \frac{1 + \gamma \tan^2\theta}{(\gamma - 1) \tan\theta} \end{aligned} \qquad (4.3\text{-}6)$$

where

$$\gamma = T_{\parallel}/T_{\perp} = \exp\left[-(a_{\parallel} - a_{\perp})L + j(\phi_{\parallel} - \phi_{\perp})L\right]$$

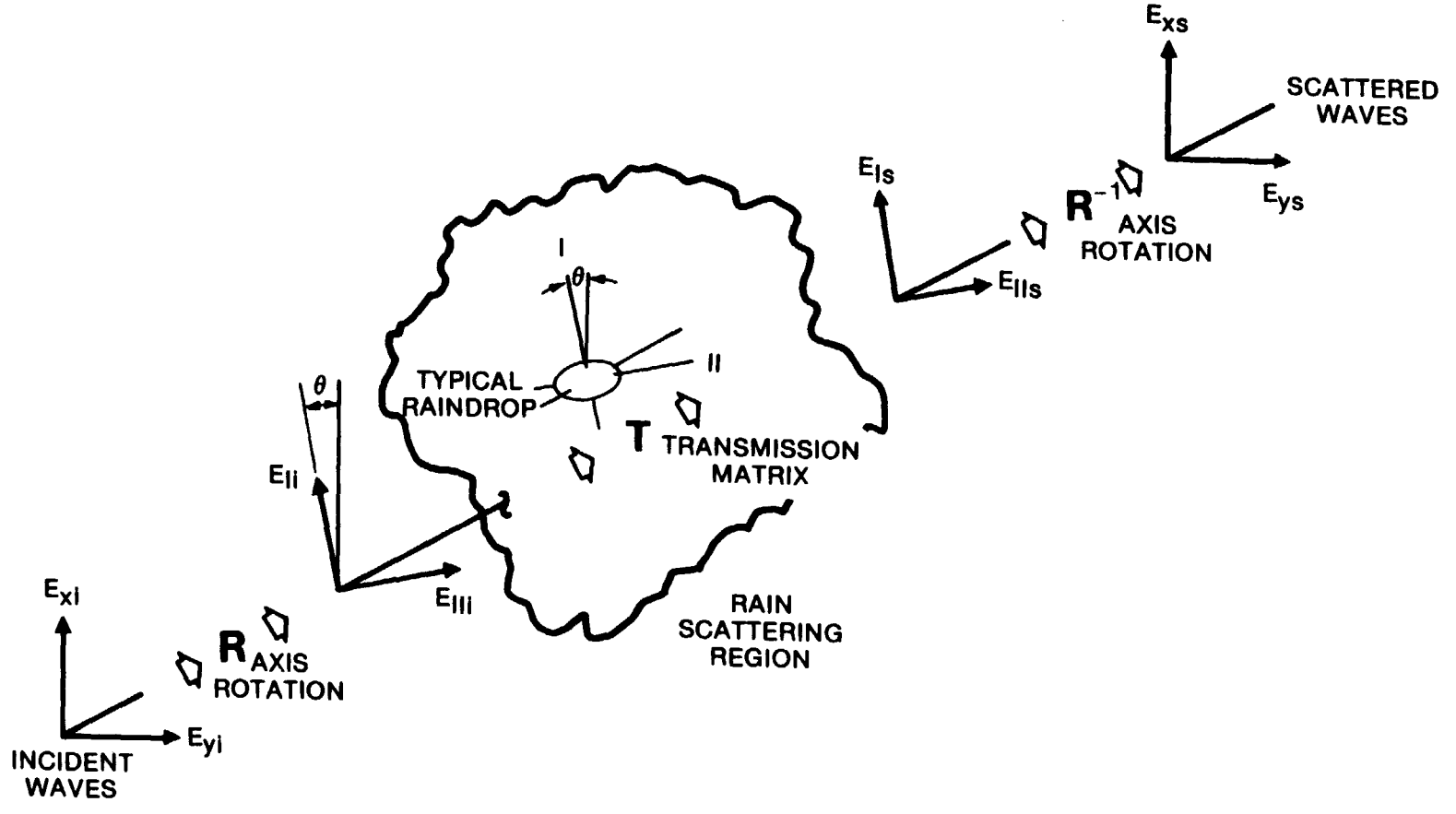


Figure 4.3-3. Components of Overall Transformation matrix T' Describing Rain Depolarization

Or, calling the y- direction the copolarized state,

$$XPD_y = 10 \log \frac{|E_{ys}|^2}{|E_{xs}|^2} \quad \text{with } E_{xi} = 0$$

$$= 10 \log \frac{|t_{yy}|^2}{|t_{xy}|^2} \qquad (4.3\text{-}7)$$

$$= 20 \log \frac{\gamma + \tan^2\theta}{(\gamma-1)\tan\theta}$$

For the case of circular polarization, Chu (1974) shows

$$XPD_c = 10 \log (|t_{xx}/t_{yx}|^2)_{\theta=45^\circ} = 20 \log \frac{\gamma + 1}{\gamma - 1} \qquad (4.3\text{-}8)$$

which is independent of the sense of rotation of the copolarized wave.

Thus far, we have assumed that all raindrops are of equal size and have the same orientation. The model must account for the distribution of sizes and shapes of raindrops and the distribution of angles $\theta$ and $\alpha$ that are present in the rain along the path. Scattering theory allows for this. The scattering effect of a single raindrop is determined as a function of some parameter (like size), then the distribution of that parameter over the population of raindrops is used in calculating the transmission coefficients. The transmission coefficients (more exactly, the specific attenuations and phase lags, A and $\bar{\Phi}$) have been calculated in this manner as a function of rain rate by several authors. The first calculations (Chu-1974, Watson and Arbabi-1973a) used oblate spheroidal raindrops. The drops were assumed to be distributed

be distributed according to the well-known Laws and Parsons distribution, and to have eccentricities that were directly related to their sizes, with the largest drops being the most deformed. Later work has considered the more realistic Pruppacher-Pitter (1971) drop shapes (Oguchi-1977). Figure 4.3-4 (from Morrison, et al -1973) is an example of the results of these calculations. These curves give the difference in the specific attenuation and phase between the I and II axes. The angle between the direction of propagation and the raindrop symmetry axis, $\alpha$ , is a parameter, and the canting angle, $\theta$, is set to 25°. The differential attenuation and phase are of most interest because they actually determine XPD. As can be seen from the curves, the worst case for differential attenuation and phase corresponds to $\alpha$ = 90°. This agrees with intuition, since the projection ellipse of the drop onto the plane containing the field vectors has the greatest eccentricity for that case. For values of $\alpha$ different from 90°, Chu (1974) shows that the following approximation is quite accurate:.

$$A_{II} - A_{I} = \sin^2\alpha \, (A_{II} - A_{I})_{\alpha = 90°} \qquad (4.3\text{-}9)$$

$$\Phi_{II} - \Phi_{I} = \sin^2\alpha \, (\Phi_{II} - \Phi_{I})_{\alpha = 90°}$$

Accounting for the distribution of $\alpha$ and $\theta$ is more difficult than doing so for drop size and shape. We have little information about the distribution of the orientation of raindrops. It is expected that wind and wind gusts produce an appreciable spatial correlation in the orientation. In the absence of wind, a fairly symmetric distribution about the vertical would be expected.

The $\alpha$ component of drop orientation is usually considered to be equal to a constant 90° for line-of-sight (horizontal) paths and the complement of the elevation angle for satellite (oblique) paths. The effect of $\alpha$ on XPD is apparently so small compared with the canting angle dependence that allowing for a distribution of $\alpha$ is not worthwhile.

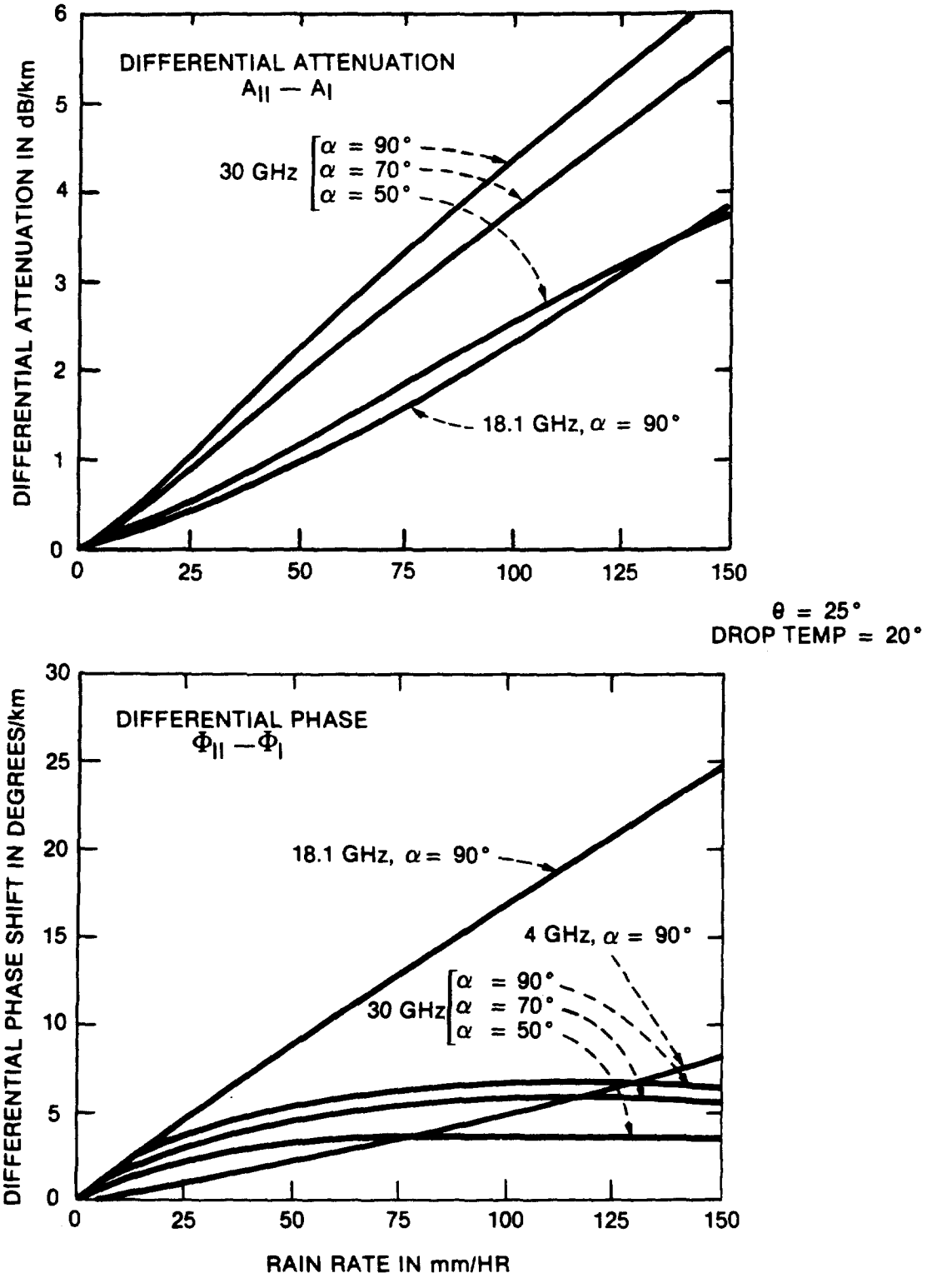


Figure 4.3-4. Differential Attenuation and Phase for Rain, From Morrison, et. al. (1973)

The canting angle distribution, as it affects XPD, has been studied extensively. Thomas (1971) presents an experimentally determined canting angle distribution and derives an "average" angle of 15°. He further notes that the crosspolarizing effects of canting angles of positive and negative sense tend to cancel, so the overall effect is proportional to the excess of one sense over the other. Based on some experimental evidence, he chooses 25% as the worst case imbalance of canting angle sense. The predicted worst case XPD, then, is roughly that produced by 25% of the raindrops at a 15° canting angle. Chu (1974) uses similar reasoning, but gives evidence that the mean canting angle is about 25°, and that the effective angle sense imbalance is about 14%. Watson and Arbabi (1973b) calculate XPD versus rain rate at 11 GHz assuming a Gaussian canting angle distribution with a non-zero mean value, and uncorrelated drop orientations. The results were nearly the same as those assuming a fixed canting angle equal to the mean value.

Distributions of both $\alpha$ and $\Theta$ can be accounted for by the following transformation (Oguchi-1977).:

$$\begin{bmatrix} a_I - j\phi_I \\ a_{II} - j\phi_{II} \end{bmatrix} = \begin{bmatrix} 1 + m_\theta m_\alpha & 1 - m_\theta m_\alpha \\ 1 - m_\theta m_\alpha & 1 + m_\theta m_\alpha \end{bmatrix} \begin{bmatrix} a_I' - j\phi_I' \\ a_{II}' - j\phi_{II}' \end{bmatrix} \qquad 4.3\text{-}10)$$

where the unprimed a's and ø's are <u>effective</u> attenuation and phase constants and the primed ones correspond to $\alpha$=90°. The canting angles and incidence angles are assumed to be randomly distributed with means $\theta$ and $\alpha$ variances $\delta_\theta^2$ and $\delta^2_\alpha$ . The transformation parameters, assuming Gaussian distributions, are

$$m_\theta = \exp\ (-2\delta_\theta^2) \qquad (4.3\text{-}11)$$

$$m_\theta = \exp\ (-2\sigma_\theta^2)$$

$$m_\alpha = \frac{1}{2}\ [1 + \exp\ (-2\sigma_\alpha^2) \sin 2\bar{\alpha}]$$

where $\sigma_\theta$ and $\sigma_\alpha$ are in radians. The effective canting angle used in the formulas for XPD, etc. is $\bar{\theta}$. Substituting the effective attenuation and phase constants a, $\phi$ into the formula for XPD (4.3-6), making the small argument approximation

$$\gamma = \exp\left[-(a_{II}'-a_I')L + j(\phi_{II}'-\phi_I')L\right]$$

$$\approx 1 - (a_{II}'-a_I')L + j(\phi_{II}'-\phi_I')L \qquad (4.3\text{-}12)$$

and making further approximations based on the known values of the a's and $\phi$'s, we arrive at

$$XPD \approx -20 \log \left\{ \frac{1}{2} m_\theta m_\alpha L\left[(\Delta a')^2 + (\phi')^2\right]^{1/2} \sin 2\bar{\theta} \right\} \qquad (4.3.13)$$

where'

$$\Delta a' = a_{II}'-a_I'$$

$$\Delta\phi' = \phi_{II}'-\phi_I'$$

This is good approximation for frequencies in the 4-50 GHz range and rain rates less then 150 mm/hr. If, in addition, we neglect the effect of the distribution of a and assume that the drops are oriented horizontally in the plane of incidence, as do Nowland, et.al. (1979), we can write

$$\sigma_\alpha^2 \ll 1$$

$$\bar{\alpha} = 90^\circ - \varepsilon \qquad (4.3\text{-}14)$$

where $\varepsilon$ is the antenna elevation angle. This implies

$$m_\alpha = \cos^2\varepsilon \qquad (4.3\text{-}15)$$

which further simplifies the approximation for XPD. The result is

$$XPD \approx -20 \log \left[ \frac{1}{2} m_\theta L |\Delta k'| \cos^2\varepsilon \sin 2\bar{\theta} \right] \qquad (4.3\text{-}16)$$

with

$$|\Delta k'| = [(\Delta a')^2 + (\Delta \phi')^2]^{1/2}$$

### 4.3.2 Relationship between Depolarization and Attenuation due to Rain

An empirical relation has been observed between the exceedance statistics for attenuation and those for XPD on the same path. The relation is

$$XPD \approx \tilde{a} - \tilde{b} \log(CPA) \qquad (4.3\text{-}17)$$

where XPD is the value of cross-polarization discrimination not exceeded for a given percentage of the time, and CPA is the copolarized attenuation value in decibels, exceeded for the same percentage of the time. The empirical constant $\tilde{a}$ is typically found to be in the 30-50 dB range and $\tilde{b}$ is usually around 20. We present below the theoretical basis supporting this relation, and examine some of the experimental evidence for it.

Referring back to Section 4.3.1, we can obtain an expression for attenuation of the copolarized wave in a manner similar to finding the XPD. The copolarized attenuation, assuming a LP incident wave oriented in the x-direction, is given by

$$\begin{aligned} CPA &= -10 \log \frac{|E_{xs}|^2}{|E_{xi}|^2} \text{ with } E_{yi} = 0 \\ &= -10 \log |t_{xx}|^2 \\ &= -20 \log |T_\perp \cos^2\theta + T_\parallel \sin^2\theta| \\ &= -20 \log |T_\perp [1 + (e^{-(\Delta a - j\Delta\phi)} - 1) \sin^2\theta| \end{aligned} \qquad (4.3\text{-}18)$$

where $\Delta a$ and $\Delta\phi$ are defined under equation (4.3-13). Using the small argument approximation (4.3-12) we can obtain

$$CPA_x \approx -20 \log [\exp(-a_I L \cos^2\theta - a_{II} L \sin^2\theta)]$$

$$= (A_I \cos^2\theta + A_{II} \sin^2\theta) L \qquad (4.3\text{-}19)$$

The same expression, with I and II subscripts interchanged, is found for $CPA_y$ . Note that the above expression applies only when all the raindrops have the same orientation. Averaging over distributions of orientation angles $\alpha$ and $\theta$, as was done earlier to find the XPD, we obtain

$$CPA_x = \frac{1}{2}[(A_I' + A_{II}') + m_\theta m_\alpha (A_I' - A_{II}') \cos 2\bar{\theta}\,]L \qquad (4.3\text{-}20)$$

where $A_I'$ and $A_{II}'$ are the attenuation coefficients, in dB/km, for $\alpha = 90^\circ$. Again assuming as before, that the raindrops are not distributed in $\alpha$, and that $\alpha = 90^\circ - \varepsilon$,

$$CPA_x = \frac{1}{2}[(A_I' + A_{II}') + m_\theta (A_I' - A_{II}') \cos^2\varepsilon \cos 2\bar{\theta}]L \qquad (4.3\text{-}21)$$

$CPA_y$ is the same except that the sign of the second term is minus.

To relate XPD and CPA, we assume that the CPA, the attenuation coefficients $A_I$ and $A_{II}$, the magnitude of the differential propagation constant, and the effective path length all bear a power law relation to the effective rain rate, R (Nowland, et al-1977):

$$CPA = a_0 R^{b_0} L \qquad (4.3\text{-}22a)$$

$$A_{I'} = a_1 R^{b_1} \qquad (4.3\text{-}22b)$$

$$A_{II'} = a_2 R^{b_2} \qquad (4.3\text{-}22c)$$

$$L = u R^{v} \qquad (4.3\text{-}22d)$$

$$|\Delta k| = c R^{d} \qquad (4.3\text{-}22e)$$

Substituting (4.3-22a-c) into (4.3-21) gives approximate expressions for $a_o$ and $b_o$ in terms of $a_1$, $a_2$, $b_1$ and $b_2$, which can be determined by regression fitting to the calculated propagation constants. The parameters u, v, c and d can also be determined by regression fitting to theoretical or empirical relations.

Substituting (4.3-22d) and (4.3-22e) into the formula for XPD, (4.3-16), gives XPD in terms of R and regression parameters. Likewise, using (4.3-22d) in (4.3-22a) gives CPA in terms of R and regression parameters. Elmininating R then relates XPD and CPA:

$$XPD \cong \tilde{a} - \tilde{b} \log CPA \qquad (4.3\text{-}23)$$

with

$$\tilde{a} = 20\left(\frac{d+v}{b_o+v}\right)\log(a_o u) - 20 \log\left(\tfrac{1}{2} c\, u\, m_\theta \cos^2\xi \sin 2\bar{\theta}\right)$$

$$\tilde{b} = 20\left(\frac{d+v}{b_o+v}\right) \qquad (4.3\text{-}24)$$

In the 11-14 GHz range, $b_o = d$, which simplifies the formulas:

$$\tilde{a} \cong -20 \log\left(\frac{1}{2a_\theta} c\, m_\theta \cos^2\xi \sin 2\bar{\theta}\right)$$

$$\tilde{b} \cong 20 \qquad (4.3\text{-}25)$$

Throughout the preceding development, linear polarization in the x direction was assumed. For LP waves in the y- direction, the l

and 2 subscripts in the formulas for $a_o$ and $b_o$ are reversed. For CP waves, 8 is set to 45°, which gives the lowest value of XPD.

The CCIR developed a provisional formula based on the above analysis, which provided a simplified form to allow for the prediction of XPD for a given percentage of the time. The CCIR formula was first presented in CCIR Report 564-1, (CCIR-1978), and later updated and modified in Report 564-3, (CCIR-1986). The CCIR formula essentially sets

$$d \cong b_o$$

$$\frac{cm_\theta}{2a_o} \approx [f(GHz)]^{-3/2} \qquad (4.3\text{-}26)$$

$\bar{\theta} \approx \tau$ = polarization tilt angle with respect to horizontal

to arrive at the "CCIR Approximation"

$$XPD = 30 \log[f(GHz)] - 40 \log(\cos \varepsilon) - 10 \log[1-.484(1 + \cos(4\tau))]$$
$$- 20 \log(CPA) + .0052\sigma_\phi^2 \qquad (4.3\text{-}27)$$

where $\sigma_\varnothing$ is the effective standard deviation of the raindrop canting angle distribution, expressed in degrees. [The CCIR prediction procedure is described in detail in Chapter VI, Prediction Techniques.]

The "exact" evaluation of the a and b coefficients requires first finding $a_1$, $b_1$, $a_2$, $b_2$, c and d by regression fitting to the parameters $A_I$, $A_{II}$, and $\Delta k$ versus rain rate and frequency. These parameters in turn are determined by the propagation constants ($a_I$, $\phi_I$, etc.) corresponding to the raindrop symmetry axes. Nowland, et

al (1977) report the results of regression calculations performed in this manner for oblate spheroidal and Pruppacher-Pitter-form raindrops, for the Laws-and Parsons drop size distribution. More extensive results are included in CCIR Document 5/206 (1977), a Canadian submission to the Study Group 5 Final Meeting. That report also contains the regression coefficients for path length, u and v. These are given as functions of elevation angle for three ranges of rain rate, and were computed based on an empirical formula for path length.

The orientation distribution of the raindrops is the rain characteristic about which we know the least. It enters into the computation in finding $a_o$ and $b_o$ from $a_1$, $a_2$, $b_1$ and $b_2$, and in finding $\tilde{a}$. As stated earlier, it is apparently quite safe to ignore the effect of the angular distribution in the plane of incidence (see Figure 4.3-1). This allows us to set $\alpha = 90^o - \varepsilon$ , the complement of the elevation angle of the path. The drop orientation angle $\theta$ with respect to the polarization direction, measured in the plane normal to the path, can be expressed as the difference $\theta = \phi - \tau$ where $\phi$ is the drop canting angle and $\tau$ is the polarization direction, both measured with respect to the horizontal. Since $\tau$ is known, it is the statistics of $\phi$ that determines $\bar{\theta}$ and $\sigma_\theta$ (or $m_\theta$ ), i.e.

$$\bar{\theta} = \bar{\phi} - \tau, \quad \sigma_\theta = \sigma_\phi \tag{4.3-28}$$

It is convenient to describe the distribution of $\phi$ by an equivalent canting angle $\phi_e$ , defined by

$$\sin 2|\phi_e - \tau| = m_\theta \sin 2|\phi - \tau| \tag{4.3-29}$$

The equivalent canting angle is the canting angle that identically oriented raindrops would need to have in order to produce the same XPD. Nowland, et al (1977) cite a measured value of $4^o$ for $\phi_e$ that is consistent with independently-determined values of $\bar{\phi}$ and $\sigma\phi$ , but give other experimental results that show little consistency. $\phi$ More work is clearly needed in characterizing the canting angle.

Chu (1980) employed a "two-tiered" Gaussian model for the canting angle. It assumes first that the instantaneous canting angle has a Gaussian distribution with mean $\phi_m$ and standard deviation $S\phi$. Second, the mean angle $\phi_m$, which varies with time, is itself assumed to be Gaussian. The distribution of $\phi_m$ has zero mean and standard deviation $S_m$ . The values of these parameters that apparently give the best agreement with experimental data are $S\phi$ = 30° and $S_m$ = 3°.

Based on this two-tiered model, Chu (1982) derived a semi-empirical formula for depolarization versus attenuation that agrees with experimental results over a wide range of frequency, polarization tilt angle and elevation angle. Cross-polarization discrimination for circular polarization $XPD_C$ , in decibels, is given by

$$XPD_C = 11.5 + 20 \log f - 20 \log (CPA) - 40 \log (\cos\varepsilon) \qquad (4.3\text{-}30)$$

where f is frequency in gigahertz, CPA is copolar attenuation in decibels, and $\varepsilon$ is elevation angle. The formula for cross-polarization discrimination with linear polarization, $XPD_L$ , in decibels, is

$$XPD_L = 11.5 + 20 \log f - 20 \log (CPA) - 40 \log (\cos\varepsilon) - 10 \log 1/2 (1 - 0.978 \cos 4\tau) - 0.075 (CPA) \cos^2\varepsilon \cos 2\tau \qquad (4.3\text{-}31)$$

where $\tau$ is the polarization tilt angle measured from the horizontal.

Note that the formulas (4.3-30) and (4.3-31) contain a frequency dependence of 20 log f. This disagrees with the provisional formula of the CCIR (Equation 4.3-27), which has a 30 log f frequency dependence. There is little discrepancy between the predictions

given by the two formulas for frequencies in the vicinity of 12 GHz, but the above formulas give better agreement with data at 19 and 28 GHz.

### 4.3.3 Statistical Characteristics of Rain Depolarization

Two models have been proposed for predicting the statistical characteristics of rain depolarization. Chu (1980) determined functional dependencies of cross polarization on frequency, polarization and elevation angle, and presented techniques for finding depolarization statistics on the basis of rain rate or rain attenuation statistics. Kanellopoulos and Clarke (1981) developed a method of predicting long-term rain depolarization statistics on short terrestrial links. The distribution of cross-polarization isolation, in decibels, turns out to be approximately Gaussian. An assumption of uniform rain rate restricts the model to short paths, but an extension to the more general case of varying rain rate along the path is in progress. The general method should also be applicable to satellite paths.

Experimental depolarization data on satellite paths appears to be approximately normally distributed. Combining this with the observed log-normal distribution of rain attenuation, a probabilistic model of depolarization in combination with attenuation has been proposed (Wallace - 1981). In this model the joint probability density of XPD, in decibels, and the logarithm of rain attenuation, in decibels, is approximated by a bivariate Gaussian density. This description agrees fairly well with experimental results. The proposed model has been used in the analysis of single-site and diversity system availability.

### 4.3.4 Experimental Depolarization Data

The most extensive experimental investigations of depolarization above 10 GHz to date have been performed at Virginia Polytechnic Institute and State University (VPI & SU) at Blacksburg (Bostian and Dent - 1979) (Stutzman et.al. - 1983), the University of Texas (UT)

at Austin (Vogel - 1978), and the Bell Telephone Laboratories (BTL) in Holmdel, and Crawford Hill, N.J. (Arnold, et al - 1979). The signal sources for depolarization measurements conducted at these facilities have been beacons on the following spacecraft.

| | |
|---|---|
| ATS-6 | 20 GHz, 30 GHz, LP |
| CTS | 11.7 GHz, RHCP |
| COMSTAR | 19.04 GHz, Vert. & Horiz. LP |
| COMSTAR | 28.56 GHz, Vert. LP |
| SIRIO | 11.6 GHz, RHCP |

Four COMSTAR spacecraft, D-1 through D-4, have been used.

In the experiments, the signal levels in the copolarized and cross polarized channels were measured, either continuously or during periods of rain. The measurement records were typically used to generate XPD and CPA statistics and plots of XPD versus CPA. Some results of these experiments are presented in section 6.7.2.

Both the VPI and SU and the UT data bases have been processed to give XPD vs CPA on an instantaneous basis, and on a statistical basis. In the former case, XPD values that were observed at the same time as the corresponding CPA value are plotted. In the latter case, the XPD value that was not exceeded for a particular percentage of time is plotted against the CPA value that was exceeded for the same time percentage. An instantaneous XPD vs CPA plot was prepared for each month, and a curve of the form $XPD = \tilde{a} - \tilde{b} \log CPA$ was fitted to it. Table 6.7-1 shows the $\tilde{a}$ and $\tilde{b}$ parameters giving the best fit for each monthly plot for the 1978 VPI and SU data. The parameter R, which indicates how well the data fits the analytical curve ($R^2 = 1$ for perfect fit), is given for each case. The best-fit $\tilde{a}$ and $\tilde{b}$ values are quite variable month-to-month, and some months have very low $R^2$ values. The UT data gave similar results. This indicates that the formula s probably not very reliable for predicting XPD versus CPA on an nstananeous basis. Statistical plots, on the other hand, generally show very